Trans. JWRI, Vol. 23 (1994), No. 2

Temper Embrittlement of Cast Duplex Stainless Steels After Long-Term Aging†

Lubos MRAZ*, Fukuhisa MATSUDA, Yasushi KIKUCHI***, Naruo, Sakamoto**** and Seiichi Kawaguchi******

Abstract

Microstructural changes and fracture behavior in cast CF8M duplex stainles steel after aging at 300 to 450°C for 300 to 10000 h have been investigated. Both, optical microscopical and transmission electron microscopical analyses, hardness and ferrite content measurements have been carried out in this study. Strengthening and overaging phenomena of the ferrite phase have been identified by hardness measurements. Spinodal decomposition and heterogeneuous precipitation of G-phase were found to be responsible for strengthening of the ferrite phase after aging with a temper parameter P in the range ca. 1.8 to 4.0. Homogeneuous precipitation of noncoherent α'- and G-phases in ferrite, identified by both optical and transmission electron microscopical analyses for aging with P > 4.0 at 450°C, is associated with overaging phenomena. Three different fracture modes, dimples, cleavage and α/γ grain boundary separation, have been observed for Charpy V-notch and CT test specimens fractured at +20°C.

KEY WORDS: (Embrittlement) (Duplex Stainless Steel) (Aging) (Microstructure Changing)

1. Introduction

Cast duplex stainless steels are widely used in the nuclear, oil and chemical industries. They exhibit excellent strength, corrosion resistance and good weldability. Good properties are shown by duplex, ferritic-austenitic microstructures, where the ferrite content is accepted up to the level of 25%. In the nuclear industry, these steels are used for primary piping systems of pressurised water reactors (PWR) designed to operate for 40 years at 290 to 330°C. The life time prediction takes into account the instability of the ferrite phase, which is supposed to undergo so-called "475°C embrittlement"[1,2]. Trautwein and Gysel[3] verified this prediction and showed that this embrittlement takes place rapidly, with an activation energy of 24 000 cal/mol and is associated with the changes of the ferrite phase. The embrittlement was proportional to the ferrite content of the tested steels (**Figure 1**). The changes in the ferrite phase were, for this type of steel, characterized by Chung and Chopra[4,5]. They found that five metallurgical processes such as spinodal decomposition, α'-precipitation, $M_{23}C_6$, γ 2 and G-phase precipitation contribute to the embrittlement. They also proposed an approximate TTT (time-temperature-transformation) diagram of the ferrite phase decomposition for temperatures below 500°C (**Figure 2**). Spinodal decomposition, α'-phase and G-phase precipitation, as thermally activated processes, are generally considered as the most important factors in the embrittlement of aged cast duplex stainless steels.

In the present work, the analysis of CF8M centrifugally cast duplex stainless steel has been performed in order to understand the embrittlement of the ferrite phase and the fracture behavior of CF8M duplex stainless steel after aging in the temperature range 300 to 450°C for 300 to 10000 h.

2. Experimental Procedure

2.1 Material Characterization

As-cast and aged CF8M duplex stainless steel, has been investigated in this study. Chemical composition and mechanical properties of this steel is given in **Tables 1 and 2** respectively. The requirements of ASTM A351/A351M specifications for CF8M material are also given in these Tables.

† Received on Nov. 25, 1994
* Forein researcher (Welding Research Institute, Blatislava, Slovakia)
** Professor
*** Associate Professor
**** Mitsubishi Heavy Industries, Ltd. (Takasago Research & Development Center)
Transactions of JWRI is published by Welding Research Institute, Osaka University, Ibaraki, Osaka 567, Japan

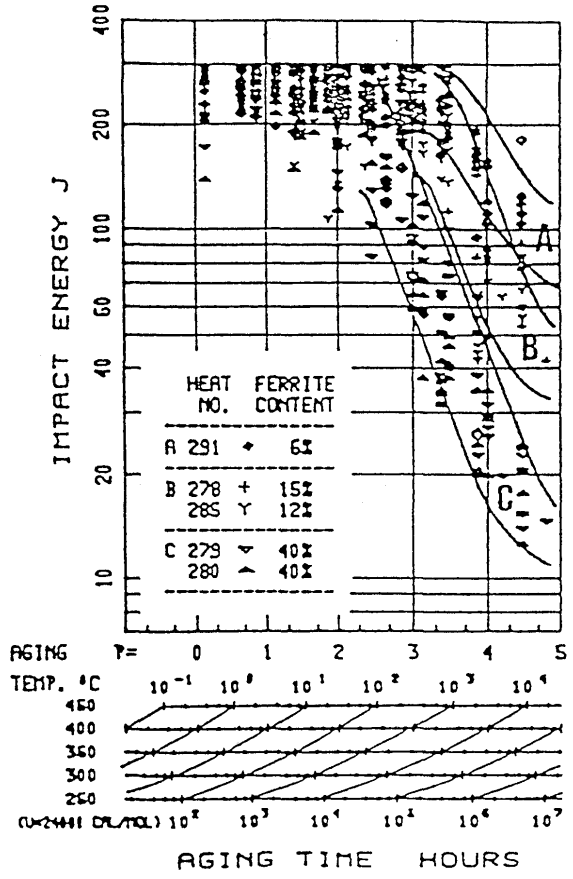

Fig. 1 Influence of ferrite content on the embrittlement of cast duplex stainless steels **(3)**

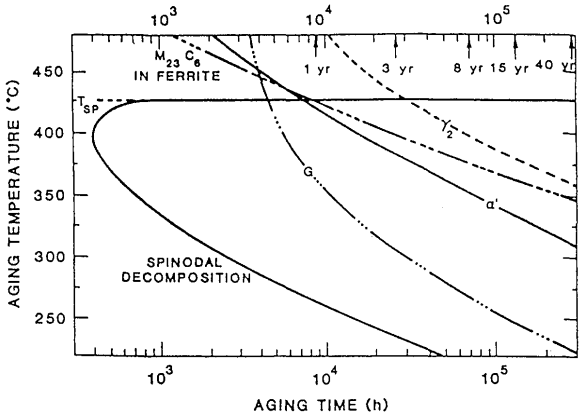

Fig. 2 Approximate TTT diagram for precipitation of G, $M_{23}C_6$, α', γ_2 and spinodal decomposition in ferrite of stainless steels during aging at 250 to 450°C **(4, 5)**

Table 1 Chemical composition of tested CF8M duplex stainless steel

	wt (%)										
	C	Si	Mn	P	S	Ni	Cr	Mo	Nb	N	O
ASTM A351	max. 0.080	max. 2.00	max. 1.50	max. 0.040	max. 0.040	9.0 12.0	18.0 21.0	2.0 3.0	-	-	-
	0.048	0.64	0.84	0.028	0.005	10.46	20.01	2.16	0.01	0.051	0.0075

Table 2 Mechanical properties of tested CF8M duplex stainless steel

	Y.S. (MPa)	U.T.S. (MPa)	A5 (%)	Z (%)
ASTM A351	min 205	min 485	min 30	-
	244	515	43.9	73.8

Charpy V-notch specimens of as-cast and aged material at 300, 350, 400 and 450°C for 10 000 h and at 300°C for 40 000 h, and CT specimens of as cast and aged at 300°C for 10000 h and at 350, 400 and 450°C for 300, 3000 and 10000 h fractured at + 20°C were analyzed. Also CT specimens of CF8M material aged at 350, 400 and 450°C for 10000 h and at 400°C for 3 000 h fractured at + 325°C were investigated.

The P-value (see APPENDIX) of aged CF8M material, considering a Cr activation energy of Q=24 000 cal/mol, was calculated in the range between 1,86 to 4,53 (**Table** 3).

Mechanical properties, Charpy V-notch and JIC values of the aged material are given in **Table 3**. The influence of aging on Charpy V-notch impact energy is shown on **Figure 3**.

2.2 Metallographic Examination

Optical, scanning and transmission electron microscopical analyses have been carried out in this investigation. Ferrite hardness and the ferrite content measurements have also been performed in order to characterize microstructural changes of the ferrite phase upon aging, and subsequent fracture behavior of the analyzed steel.

2.3 Optical Microscopical Analysis

Microstructures of as-cast and aged CF8M duplex stainless steel have been revealed by the following etchants: 10% NaOH solution in water, 10% HCl solution

Table 3 Mechanical properties, impact energy and fracture ductility of as-cast and aged CF8M duplex stainless steel

aging		P	Y.S.	U.T.S.	elongation	reduction	impact	fracture ductility
temperature (°C)	time (h)		(MPa)	(MPa)	(%)	(%)	(J)	J_{IC} (kJ/m²)
300	0	0	237 250	515 515	44.0 43.8	74.6 73.0	321 276	(2265) (2305)
	10000	2.65	274 253	559 549	45.0 45.4	77.6 67.7	287 264	(2206) (2373)
350	300	1.86	239 265	539 552	38.0 43.0	73.6 79.8	293 278	(2903) 1540
	3000	2.86	244 267	588 588	36.0 41.0	75.1 69.8	194 129	922 941
	10000	3.38	259 256	617 594	36.0 36.0	58.3 61.6	105 87	569 500
400	300	2.48	239 264	556 564	39.0 38.0	78.4 72.0	222 222	1393 785
	3000	3.48	257 261	598 595	33.8 39.0	65.9 68.7	104 100	883 726
	10000	4.00	250 258	637 620	39.0 41.0	59.2 62.4	85 93	422 265
450	300	3.01	243 252	586 586	38.6 46.2	78.4 73.0	159 151	912 500
	3000	4.01	241 251	625 612	38.8 40.0	61.1 62.3	105 82	716 402
	10000	4.53	246 249	612 612	38.0 33.0	54.4 61.7	69 72	647 294

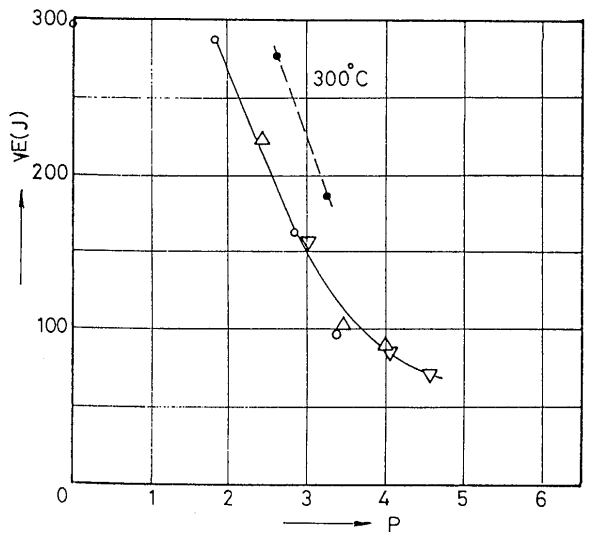

Fig. 3 Charpy V-notch impact energy of aged CF8M duplex stainless steel at +20°C

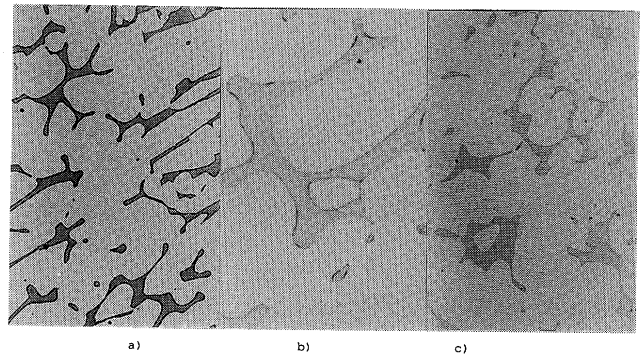

Fig. 4 Microstructure of as cast and aged CF8M duplex stainless steel
a) as cast b) aged 400°C for 10000 h
c) aged 350°C for 10000 h
a) and c) etched in 10% NaOH ×200
b) etched in glyceregia ×500

in ethyl alcohol and 10% oxalic acid in water electrolytically at 10 V and in glyceregia (glycerol+HCl+HNO_3 in volume ratio 1:1:1) and Kalling's reagent.

The microstructure of as-cast CF8M material, revealed by etching in 10% NaOH is shown on **Figure 4a**. Dark ferrite phase is homogeneuously distributed in the light austenite phase. The presence of particles (most probably $M_{23}C_6$) on the α/γ grain boundaries were found for as-cast as well as for aged CF8M material with P-values equal and less than 4 (**Figure 4b**). A gradual reduction of the contrast between ferrite and austenite phases has been revealed when etching with 10% NaOH at increasing P-values (**Figure 4a and 4c**). No change of

Table 4 Ferrite hardness and ferrite content measurements of as-cast and aged CF8M duplex stainless steel

aging		P	ferrite hardness	ferrite content		Δf
temperature (°C)	time (h)		HV 0.01	metallo (%)	ferritoscope (%)	
300	0	0	288	15.2	15.2	0
	10000	2.65	304	16.6	15.1	1.5
	40000	3.25	454	-	-	-
350	300	1.86	299	17.5	15.4	2.1
	3000	2.86	447	17.3	15.4	1.9
	10000	3.38	514	17.1	15.5	1.7
400	300	2.48	345	17.7	15.1	2.6
	3000	3.48	471	16.7	13.2	3.5
	10000	4.00	639	17.3	13.2	4.1
450	300	3.01	442	16.7	14.2	2.5
	3000	4.01	564	16.8	11.6	5.2
	10000	4.53	538	15.2	9.4	5.8

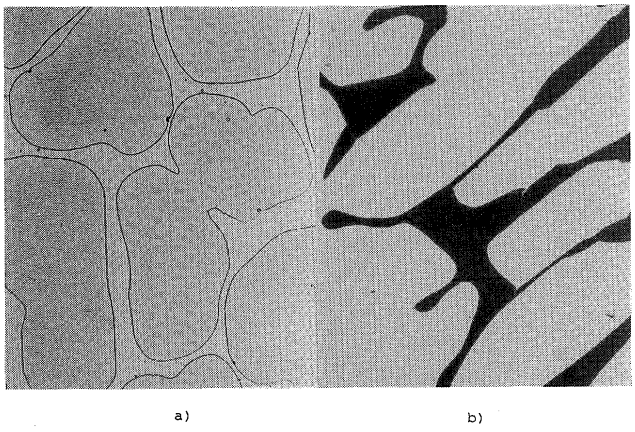

Fig. 5 Microstructure of as cast and aged CF8M duplex stainless steel
a) as cast × 500
b) aged 450°C for 10000 h etched in 10% HCl

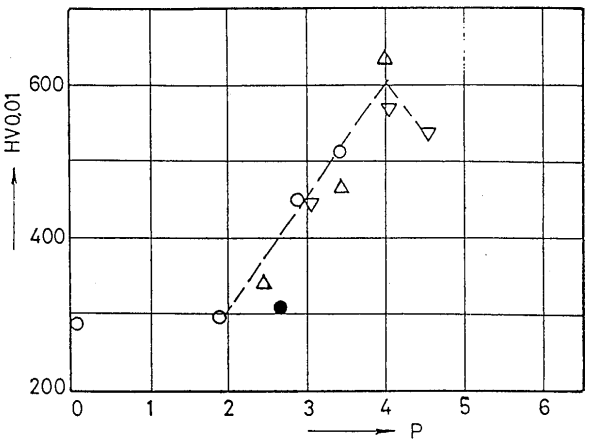

Fig. 6 Ferrite hardness HV 0.01 of aged CF8M material versus temper parameter P

microstructure has been observed with aging at P-values equal or less than 4, but intensive attack of the ferrite phase has been revealed for P-values more than 4 (aging at 450°C for 3 000 and 10 000 h) using other etchants (**Figure 5a, b**).

2.4 Ferrite Hardness Measurements

Vickers hardness of the ferrite phase has been measured with a load of 0.098 N (HV 0.01). Hardness number has been estimated as an average value of 10 indentations for as-cast and aged material. The measured values are summarized in **Table 4** and shown on **Figure 6** versus P-value. Elevation of the ferrite hardness from ca. 300 to 632 HV 0.01 of aged material with P-value in the range 1.86 to 4.00 has been measured. Drop of hardness, indicating overaging, has been observed for material aged at 450°C for 3 000 and 10 000 h (P=4.01 and 4.53). The hardness values and conditions for overaging are summarized in time-temperature diagram (**Figure 7**). Numbers in brackets indicate the hardness number and without brackets the Charpy V-notch impact energy at +20°C. Approximate isohardness lines and the P=const lines are shown in this diagram. It can be seen that hardness values of the ferrite phase are proportional to the level of impact energy of aged material.

2.5 Ferrite Content Measurements

The ferrite content of as-cast and aged CF8M material has been carried out metallographically by point counting analysis and by Ferritoscope measurement. Point counting analysis has been performed according to the ASTM standard. Altogether 25 fields were analyzed at magnification × 200 using a rectangular grid containing 70 points. The ferrite content was estimated from an average of 25 values. The results are summarized in **Table 4**. Ferrite contents in the range of 15 to 17% have been measured. No relationship has been found between the ferrite content measured by point counting and aging conditions.

The Fischer Ferritoscope, type FE8e3, was also used for the estimation of the ferrite content of as-cast and aged CF8M material. Altogether six measurements have been performed for each combination of material conditions and subsequently the average value has been calculated. The results of the measurements are summarized in Table 4 and shown on **Figure 8**. The ferrite content, which in this case represents magnetic permeability, continuously decreases for aging temperatures of 400 and 450°C. No change in the ferrite content (magnetic permeability) has been measured for aging temperature <350°C and aging times up to 10 000 h compared to that of as-cast material.

2.6 Fracture Behavior

Fracture behavior of as-cast and aged CF8M duplex stainless steel has been investigated using Charpy V-notch and CT test specimens. Both optical microscopic and scanning electron microscopic analyses were carried out in this investigation.

2.7 Charpy V-notch Specimens

Longitudinal cross section Charpy specimens, cut in the center and perpendicular to the fracture surface, were prepared for optical microscopic analysis. The microstructure close to the fracture has been analyzed. Heavy plastic deformation and voids in the austenite phase have been found in the vicinity of the fracture for as-cast specimen and specimens aged at 300°C (**Figure 9a**). Twinning and also secondary cracks were observed for specimens aged at 350 and 400°C for 10 000 h (**Figure 9b**).

The results of the fracture analysis of Charpy V-notch specimens fractured at +20°C are schematically summarized in **Figure 11** as a time-temperature diagram. The regions of the different fracture modes and also of overaging conditions for CF8M steel are drawn in this diagram.

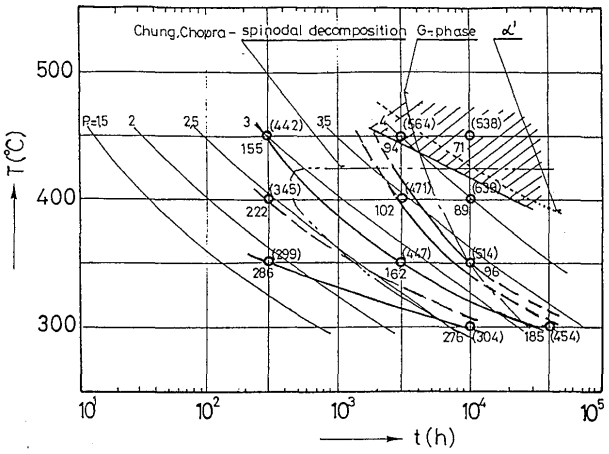

Fig. 7 Ferrite hardness, approximate isohardnes lines, overaging region of aged CF8M material in time-temperature diagram and Chung, Chopra (4, 5) prediction of spinodal decomposition, G- and α'-phase precipitation)

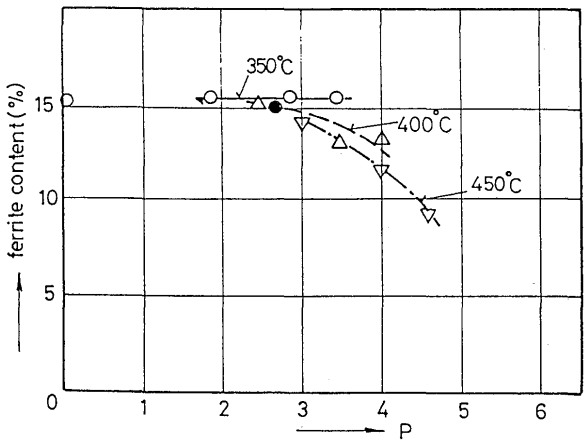

Fig. 8 Ferrite content of aged CF8M material measured by Ferritoscope

Fully ductile fracture has been observed for as-cast and specimens aged at 300°C. Dimples of ductile fracture and cleavage facets of brittle fracture were found on the fracture surface of specimens aged at 350 and 400°C (**Figure 10**). Cleavage facets contain a number of tongues on the surface with specific crystallographic orientation. Dimples of ductile fracture, cleavage facets of brittle fracture in ferrite and α/γ grain boundary separation were identified on the fracture surface of specimens aged at 450°C.

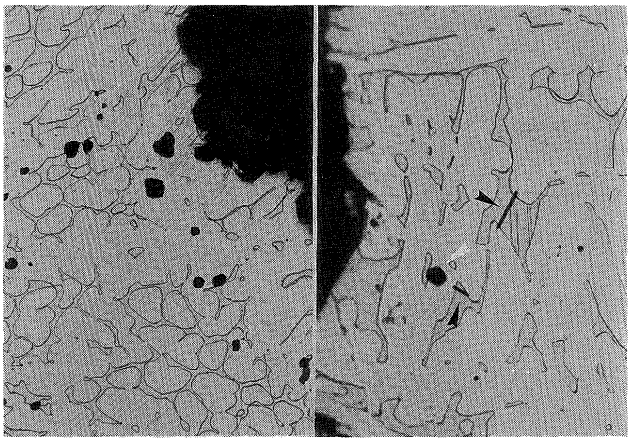

Fig. 9 Microstructure in the vicinity of the fracture of aged CF8M material
Charpy V-notch specimen fractured at +20°C
a) Plastic deformation and voids in the vicinity of fracture (as-cast)
b) Twins and secondary cracks in ferrite (aged 350°C/10000h)

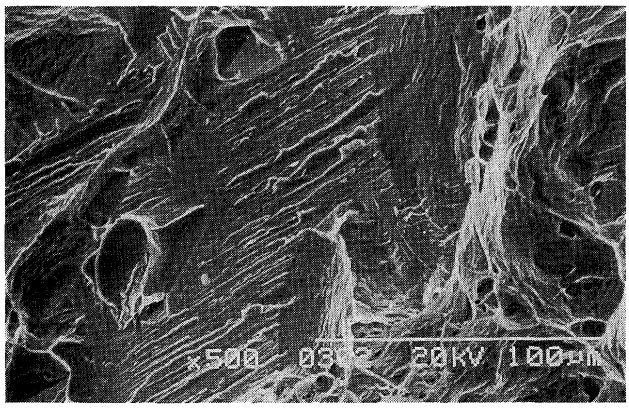

Fig. 10 SEM picture, Cleavage in ferrite
Charpy V-notch specimen of CF8M material aged at 300°C for 40 000 h fractured at +20°C

2.8 CT Test Specimens

Three different fracture modes were recognized on the surfaces of the specimens fractured at +20°C: dimples of ductile fracture, cleavage of brittle fracture and α/γ grain boundary separation (**Figure 12**). The observed fracture morphology is schematically summarized on **Figure 13** in a time-temperature diagram. In this Figure the regions of non- and overaging, as the result of hardness measurements, and also the Chung[4] prediction of spinodal decomposition are indicated. A good fit can be seen between the Chung prediction and the occurence of

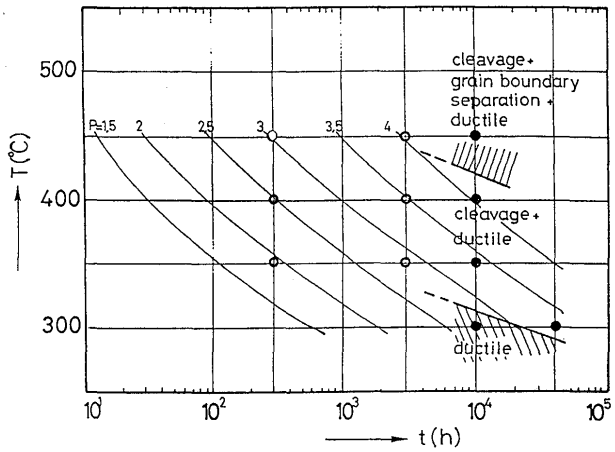

Fig. 11 Fracture morphology of aged CF8M material in time-temperature diagram
Charpy V-notch specimans fractured at +20°C

brittle fracture. Two fracture modes, ductile and α/γ grain boundary separation were observed for specimens prepared from overaged CF8M material and fractured at +325°C (**Figure 14**). Only ductile fracture has been found for nonoveraged material fractured at this temperature.

Fractographic analysis of both Charpy V-notch and CT specimens showed that the observed fracture mode of aged CF8M is for both tests similar. For both, α/γ grain boundary separation was only found for overaged material and cleavage for material aged with P> ca. 2.7.

3. Transmission Electron Microscopy

Transmission electron microscopical (TEM) analysis has been carried out by JEOL 1200FX electron microscope with an accelerating voltage of 200 kV. Carbon extraction replicas and thin foils have been used for the investigation.

Carbon extraction replicas were prepared from overaged CF8M material. The specimens were etched electrolytically in 10% HCl solution in ethyl alcohol at 10 V prior to shadowing by carbon.

Thin foils were preperad by jet polishing in STRUERS equipment using 95% acetic acid + 5% perchloric acid electrolyte at 20 to 40 V.

Two basic features of the ferrite phase substructure have been identified by the analysis of thin foils in aged CF8M material. First, so-called mottled image (**Figure 15a**), typically with contrast variations and second, the presence of a large phase, homogeneously distributed in ferrite for CF8M material aged at 450°C for 3000 and 10000 h (**Figure 15b**). The large phase has been

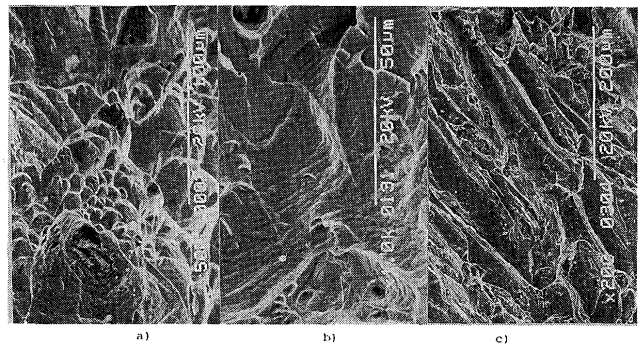

Fig. 12 SEM picture, Fracture morphology of aged CF8M material CT test specimens fractured at +20°C
a) ductile fracture
b) brittle and ductile fracture
c) ductile, brittle and grain boundary separation

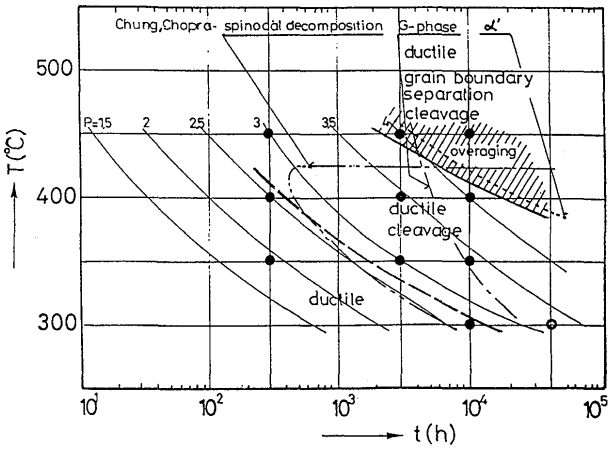

Fig. 13 Fracture morphology of aged CF8M material in time-temperature diagram
CT test specimans fracture at +20°C

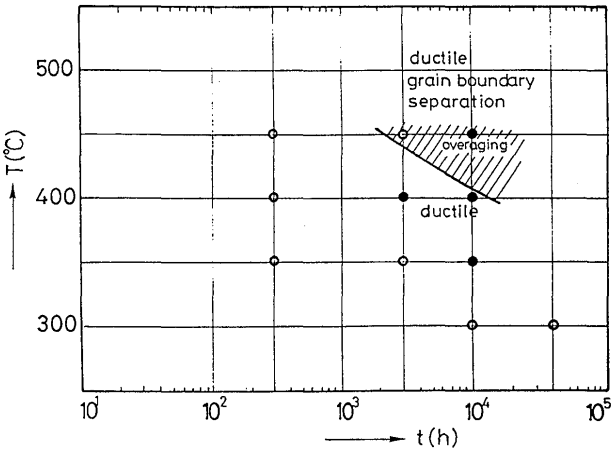

Fig. 14 Fracture morphology of aged CF8M material in time-temperature diagram
CT test specimans fracture at +325°C

identified by Ed analysis as G-phase **Figure 15c**. Dark field image of this phase from the reflection type of (333) is shown on **Figure 15d**. The presence of G-phase has been observed also for aging at 350 and 400°C for 10000 h.

The microstructure of ferrite region in CF8M material aged at 450°C for 3000 h (overaging) is shown on **Figure 16a**. Two phases are recognized, one is finer, size ca. 5 nm and second, larger, size ca. 50 nm, ordered in strings.

Electron diffraction (ED) analysis of the finer phase showed ring diffraction patterns, identified as the pattern of b.c.c. crystal structure of the α-iron phase (**Figure 16b**). Energy dispersive spectral (EDS) analysis has been performed in order to identify the chemical composition of this phase. The results are shown on **Figure 16c**. The following composition has been found: ca. 1.8% Si, 83.7% Cr, 11.0% Fe, 0.8% Ni, 3.2% Mo. From the high Cr content and the results of ED analysis we conclude that the finer phase is Cr-rich α'-phase.

ED analysis of larger phase was not possible because of its large thickness and the very high density of extracted particles. Only EDS analysis of this phase has been performed. The results are shown on **Figure 17** and the following chemical composition detected: ca. 16.8% Si, 31.7% Cr, 17.8% Fe, 19.6% Ni and 14.1% Mo. The content of Si and Ni indicate that this phase is most probably G-phase.

The results of TEM observation are summarized in time-temperature diagram on **Figure 18** and compared with Chung and Chopra's[4, 5] prediction. The regions were identified, where the mottled image, G-phase and α'-phase had been observed by TEM analysis in this investigation.

4. Discussion

The purpose of this study was to understand the microstructural changes and fracture behavior of as-cast and aged CF8M duplex stainless steel.

Optical microscopical analysis revealed that analyzed as-cast CF8M duplex stainless steel has a ferritic-austenitic microstructure with the ferrite content of ca. 15% (measured by point counting method and also by Ferritoscope) and the presence of particles, most probably a form of $M_{23}C_6$, on α/γ grain boundaries (**Figures 4a, b, c**).

Continuous changes in the ferrite phase of aged CF8M material have been revealed by several

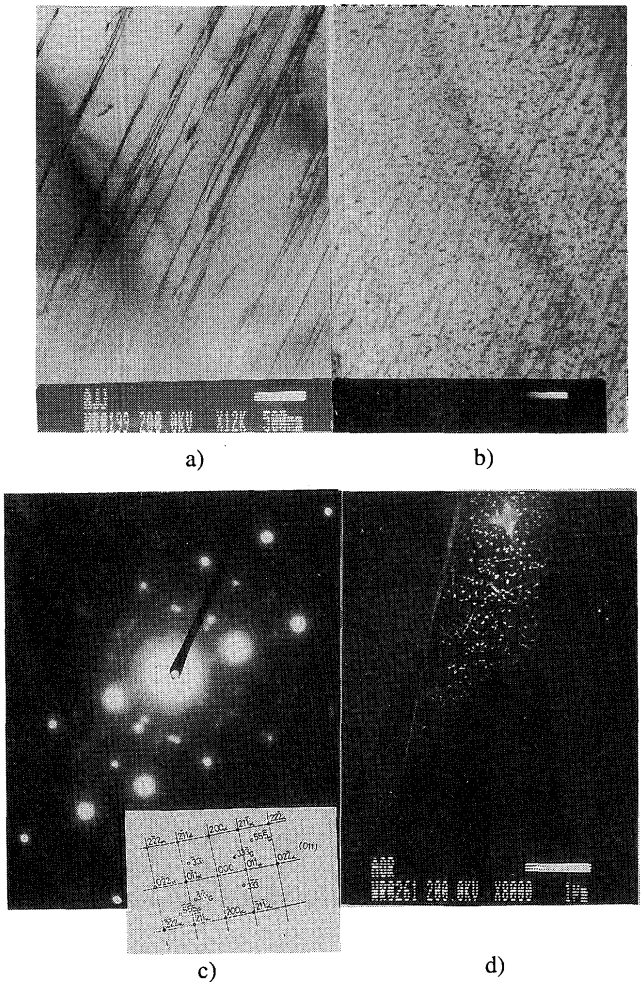

a) b)

c) d)

Fig. 15 TEM picture thin foil
a) mottled image in ferrite of CF8M aged at 400°C/10000h
b) G-phase in ferrite of CF8M aged at 450°C/3000 h
c) electron diffraction pattern of (b)
d) dark field image in reflection type (333)

independant analyses such as optical microscopical analysis, hardness and Ferritoscope measurements.

Optical microscopical examination of aged CF8M material has showed two specific features of the microstructure:

- continuous **reduction in the contrast** between the ferrite and austenite phases with increasing the level of temper parameter P when electrolytically etching in 10% NaOH (**Figures 4a, b**) and
- extensive **precipitation** in the ferrite phase of aged material with P-value more than 4 (**Figure 5b**) revealed by etchants, such as 10% HCl, 10% oxalic acid, glyceregia or Kalling's reagent.

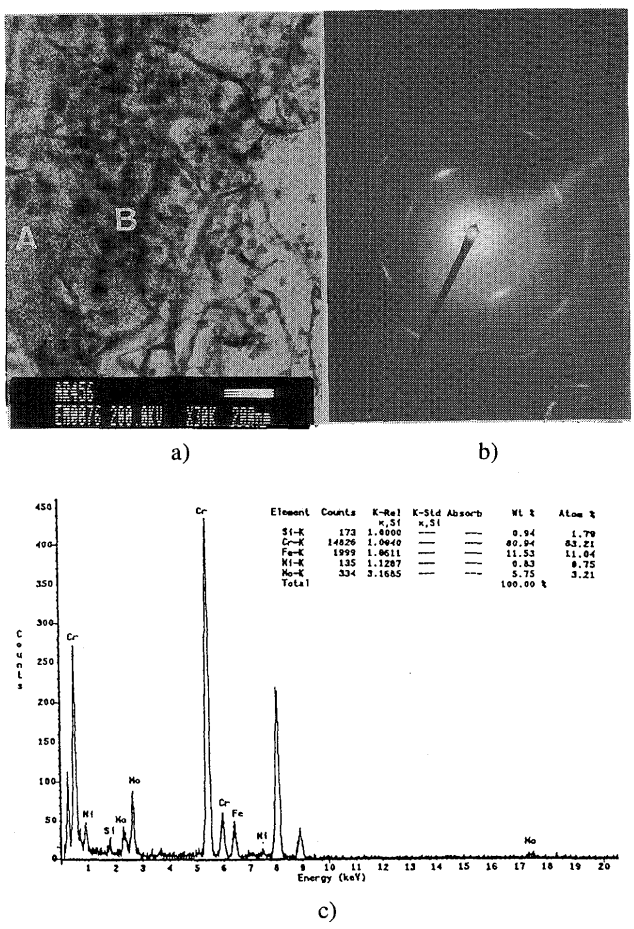

a) b)

c)

Fig. 16 TEM picture carbon extraction replica
a) α' (A) – and G (B)-phase in ferrite of aged CF8M at 450°C for 3000h
b) electron diffraction pattern of α'-phase
c) EDS analysis of α'-phase

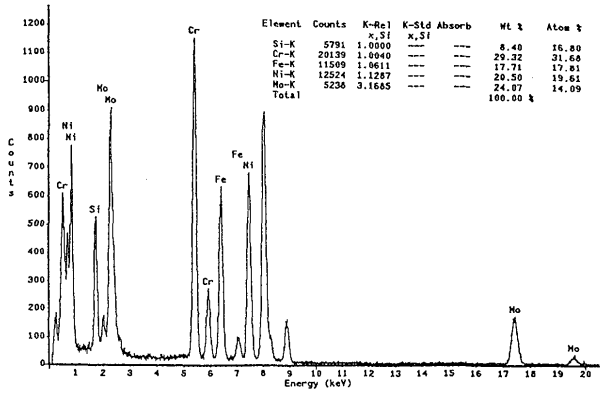

Fig. 17 EDS analysis of G-phase in ferrite of CF8M aged at 450°C for 3 000 h

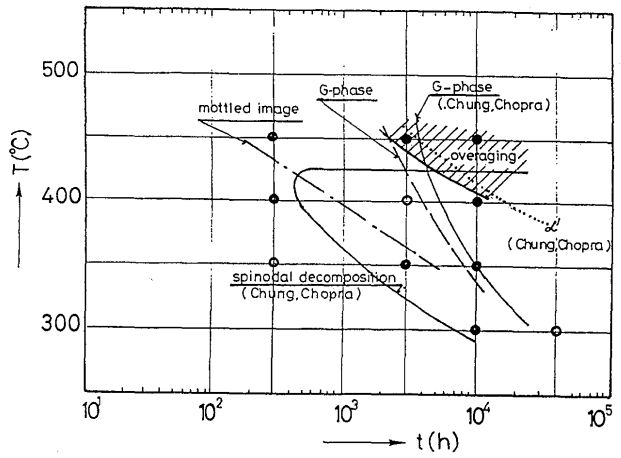

Fig. 18 Approximate time-temperature-transformation diagram of analyzed aged CF8M material estimated in this study and prediction of Chung, Chopra **(4, 5)**

The surprisingly small difference in P-value (0.01) for aging at 450°C for 3000 h (P=4.01) and at 400°C for 10 000 h (P=4.00) was associated with remarkable differences in the microstructure morphology.

Hardness measurements of aged CF8M material showed a maximum 632 HV 0.01 after aging at 400°C for 10 000 h (P=4.00). For aging with P less than 4 **continuous strengthening** of ferrite from ca. 300 HV 0.01 to 632 HV 0.01 and for aging with P > 4.00 **softening** to the level ca. 530 HV 0.01 (P=4.53) have been observed. Both, strengthening and softening, indicate that **precipitation and overaging phenomena** in the ferrite phase are responsible for observed changes. Optical microscopic analysis could identify the microstructural changes, caused by overaging, very clearly. It shows that extensive precipitation of noncoherent phase or phases is associated with overaging of CF8M material. Conversely, no change of the microstructure, revealed by most of etchants, can be recognized by optical microscopic analysis for aging with P=2 to 4.

A continuous drop in the ferrite content from 15% to 9% has been measured by Ferritoscope after aging at 400 and 450°C (**Figure 8**). These results should be evaluated carefully. The ferritoscope indicates the change of magnetic permeability and not directly the ferrite content. As was shown by optical microscopic analysis aging does not have an influence on the amount of the ferrite phase. No changes are expected in austenite at such low temperatures. It means, that the change of magnetic properties is directly associated with metallurgical changes in the ferrite phase.

The purpose of the TEM investigation was to recognize the nature of the metallurgical changes, observed by optical microscopic analysis, hardness and the ferrite content measurements.

TEM analysis of non-overaged material in thin foils revealed the presence of so-called mottled image in the ferrite (**Figures 15a**). This type of image is typical with wavy contrast which was more pronounced for aging with higher P-values. No streaks on diffraction pattern or other specific features indicating either coherent or semicoherent precipitation, have been recognized. Considering the observation of Chung and Chopra **(4, 5)**, we assume that mottled image is associated with segregation of Fe and Cr due to spinodal decomposition in the ferrite phase. ED analysis of aged material at 350 and 400°C for 10 000 h revealed also the presence of G-phase. In this case, precipitation is most probably heterogeneous, on or near dislocations.

TEM analysis of overaged material (P>4.00) revealed, that the overaging phenomenon is associated with the homogeneuous precipitation of α'- and G-phase.

The presence of α' has been identified not only by ED (electron diffraction) analysis but by EDS (energy dispersive spectral) analysis as well. The chemical composition of α' is in a good agreement with the literature data **(2)**. The observed phase seems to have size of less than 5 nm and is homogeneuously distributed in ferrite. G-phase, at ca. 50 nm, is also homogeneuously distributed in ferrite (**Figures 15b**).

The results of this analysis fit reasonably with the predictions of Chung and Chopra **(4)** (**Figure 18**). According to the results of this study, precipitation of α'-, and G-phase, has been observed for shorter aging times and the presence of mottled image, as a consequence of spinodal decomposition, for longer aging times. We assume that these differences are most probably caused by either different chemical compositions of tested material (precipitation of α'-, and G-phase) or by personal estimation (mottled image).

The analysis of the fracture behavior of as-cast and aged CF8M material showed that fracture of Charpy V-notch and CT specimens at +20°C is associated with three different fracture modes:

- dimples of ductile fracture,
- cleavage facets of brittle fracture in ferrite and
- α/γ grain boundary separation.

Ductile fracture is specific feature for material aged with P < ca. 2.7, a mixture of ductile and brittle fracture for aging with P < 4 and mixture of ductile, brittle fracture and α/γ grain boundary separation for P>4 (**Figure 13**). These results show, that brittle fracture of the ferrite phase appears for aging with P approximatelly

2.7, when the ferrite hardness exceeds the level of 350 HV 0.01 (**Figure 7**). These aging conditions also corespond with the start of spinodal decomposition proposed by Chung and Chopra (Figure 7). It means that loss of the ferrite ductility can be related to spinodal decomposition of the ferrite phase. The role of G-phase for this range of aging conditions is not yet clear.

Specific features of the ferrite brittle fracture are **twins** in the vicinity of cleaveage facets and **markings** on cleaveage facets (**Figure 10**). These markings are associated with cleavage across microtwins formed during plastic deformation. This shows that twinning plays an important role in the brittle fracture initiation.

The occurence of α/γ grain boundary separation is associated with the fracture of overaged CF8M material not only at 20°C but at 325°C as well. Most probably, the nature of strengthening via homogeneuous precipitation of noncoherent α'- and G- phases is the cause of this fracture mode.

The presence of other phases, such as $M_{23}C_6$ or $\gamma 2$ have not been clearly identified in this investigation.

5. Conclusions

Extensive metallographic examination, carried out by optical microscopical, scanning and transmission electron microscopical analyses, hardness and ferrite content measurements, has been preformed in this study. The influence of aging at temperatures in the range of 300 to 450°C for 300 to 10 000 h on microstructural changes and fracture behavior has been analyzed. It has been observed that aging is responsible for:

- strengthening of the ferrite phase for aging with P=1.86 to 4.00,
- overaging for aging with P>4.00 at temperature 450°C,
- continuous drop of magnetic permeability for aging at 400 and 450°C.

Strengthening is caused by spinodal decomposition and heterogeneuous precipitation of G-phase and associated with the occurence of cleavage fracture in Charpy V-notch and CT tests at +20°C.

Overaging is a result of homogeneuous, noncoherent precipitation of α' and G-phase and is associated with the occurence of α/γ grain boundary separation in Charpy V-notch and CT tests. Both phases were identified by electron diffraction and energy dispersive analysis.

In Charpy V-notch and CT tests at +20°C both, dimples and cleavage are fracture modes typical for nonoveraged material and a mixture of dimples, cleavage and α/γ grain boundary separation with overaged CF8M duplex stainless steel.

Literature

1) Fisher R.M., Dulis E.J., Caroll K.G.: Trans. of AIME, Journal of Metals, May, 1953, pp. 690-695
2) Grobner P.S.: Met. Trans., Vol. 4, 1, 1973, pp. 251-260
3) Trautwein A., Gysel W.: Stainless Steel Castings, ASTM STP 756, V.G. Behal and, A.S. Melilli, Eds., ASTM, 1982, pp. 165-189
4) Chung H.M., Chopra O.K.: in "Properties of stainless steels in elevated temperature service", (ed. M. Prager), PVP-ASME Vol. 132, MPC Vol. 26, 17; 1987, New York, ASME/Material Properties Council
5) Chung H.M., Chopra O.K.: in "Environmental Degradation of Material in Nuclear Power Systems-Water Reactors", August 30 – September 3, 1987, Traverse City, MI

Appendix

The degree of embrittlement is mostly characterized in terms of Charpy-V-notch impact energy using an Arrhenius extrapolation of laboratory test at higher temperatures. The aging time to reach a given degree of embrittlement at different temperatures is determined from equation

$$t = 10P \cdot \exp[Q/R(1/T - 1/673)] \quad (1)$$

where

Q – activation energy of Cr (cal/mol); T – temperature (K); R – gas constant (2 cal/mol); P – temper parameter

The P value of 1 is given to aging temperature 400°C and aging time of 10 hours.